STATISTICS, OPTIMIZATION AND INFORMATION COMPUTING
Stat., Optim. Inf. Comput., Vol. **14**, September 2025, pp 1406–1418.
Published online in International Academic Press (www.IAPress.org)

Numerical Modeling of Natural Convection in a Square Cavity Filled with Air: Fractional Derivative Formalism

Fadwa ZAROUAL*, Anass BENDARAA, Rachid FAKHAR

Laboratory LS2M (FPK), University Sultan Moulay Slimane, 25000 Khouribga, Morocco

Abstract This paper presents a numerical study of natural convection using the fractional derivative formalism. The model adopts nonlinear axis transformations and applies the finite difference method for spatial and temporal discretization in a square cavity filled with an incompressible fluid with a Prandtl number of $Pr = 0.71$. The configuration consists of four rigid walls, subjected to a temperature gradient, which serves as the driving force behind the convection. No-slip and constant temperature conditions are applied on the walls. The governing equations are solved using fractional-order operators. Isotherms and streamlines are used to visualize the results, and the influence of varying the order of the fractional derivatives is analyzed to capture fine-scale flow and heat transfer features.

Keywords Natural convection; Incompressible flow; Fractional derivative; Finite difference method

AMS 2010 subject classifications: 76M20, 76D05

DOI: 10.19139/soic-2310-5070-2576

1. Introduction

The study of natural convection in enclosures has attracted considerable attention from both academia and industries, especially in energy systems. This interest stems from its relevance in applications such as building thermal management, electronics cooling, and solar collectors [1, 2, 3].

One fundamental configuration is the square cavity, where the flow behavior is governed by the thermal boundary conditions and fluid properties. The key parameters controlling this process are the Prandtl number (Pr) and the Rayleigh number (Ra). In this study, air is selected as the working fluid ($Pr = 0.71$), and the analysis is carried out for Rayleigh numbers ranging from 10^4 to 10^6 [4, 5].

While classical models using integer-order derivatives (e.g., Navier-Stokes and energy equations) have been widely used to study natural convection, they sometimes fail to capture complex phenomena involving non-locality and memory effects. To address this limitation, we introduce a fractional-order formulation of the governing equations, extending the classical approach and enabling the modeling of anomalous diffusion and temporal persistence in the flow field [6, 7, 8].

Fractional calculus generalizes the concept of derivatives and integrals to non-integer orders, offering a powerful tool to describe systems with memory and spatial heterogeneity [9, 10]. Recent studies have shown that fractional differential equations are particularly effective in capturing both transient and steady-state behaviors in heat transfer and fluid dynamics problems [11].

*Correspondence to: FADWA ZAROUAL (Email:fadwa.zaroual@usms.ma). LS2ME polydisciplinary faculty of Khouribga Sultan Mly Slimane University 25000, Morocco).

ISSN 2310-5070 (online) ISSN 2311-004X (print)

2. Mathematical Background

In fractional calculus, the traditional differential operator D^n is extended to non-integer orders $\alpha \in \mathbb{R}$. Two commonly used definitions are the **Riemann–Liouville** and **Caputo** fractional derivatives [11].

2.1. Riemann–Liouville Derivative

$$\mathcal{D}_a^\alpha f(t)_{\mathrm{RL}} = \frac{1}{\Gamma(n-\alpha)} \frac{d^n}{dt^n} \int_a^t \frac{f(x)}{(t-x)^{\alpha-n+1}}\, dx, \quad \alpha \in (n-1, n).$$

2.2. Caputo Derivative

$$\mathcal{D}_a^\alpha f(t)_{\mathrm{Caputo}} = \frac{1}{\Gamma(n-\alpha)} \int_a^t \frac{f^{(n)}(x)}{(t-x)^{\alpha-n+1}}\, dx, \quad \alpha \in (n-1, n).$$

2.3. Relationship Between Caputo and Riemann–Liouville

$$\mathcal{D}_a^\alpha f(t)_{\mathrm{RL}} = \mathcal{D}_a^\alpha f(t)_{\mathrm{Caputo}} + \sum_{k=0}^{n-1} \frac{f^{(k)}(a)(t-a)^{k-\alpha}}{\Gamma(k+1-\alpha)}, \tag{1}$$

2.4. L1 Discretization Scheme (for $0 < \alpha < 1$)

Starting from the Caputo definition and using a piecewise linear approximation:

$$u'(s) \approx \frac{u(t_{j+1}) - u(t_j)}{\Delta t},$$

we obtain the L1 scheme:

$$\widetilde{\mathcal{D}}_t^\alpha u(t_{k+1}) \approx \frac{\Delta t^{-\alpha}}{\Gamma(2-\alpha)} \sum_{j=0}^{k} b_{j,k} \big[u(t_{j+1}) - u(t_j)\big], \tag{2}$$

where $b_{j,k} = (k+1-j)^{1-\alpha} - (k-j)^{1-\alpha}$.

2.5. L2 Discretization Scheme (for $1 < \alpha < 2$)

From the second-order Caputo derivative:

$$u''(s) \approx \frac{u(t_{j+1}) - 2u(t_j) + u(t_{j-1})}{\Delta t^2},$$

the L2 scheme becomes:

$$\mathcal{D}_{t_0}^\alpha u(t_{k+1}) \approx \frac{\Delta t^{-\alpha}}{\Gamma(3-\alpha)} \left[u(t_{k+1}) - 2u(t_k) + u(t_{k-1})\right]. \tag{3}$$

These numerical schemes provide accurate and efficient tools for discretizing fractional derivatives, enabling simulations of convection problems with memory and non-local transport properties [12, 13, 14].

3. Description of the problem and mathematical analysis

Consider a "L=1" square chamber (Figure 1). Initially,when the cavity is at temperature T_c, it is filled with an incompressible and Newtonian fluid with a Prandtl number of ($Pr = 0.71$). The horizontal walls of the cavity are assumed to be adiabatic. A horizontal temperature gradient is created because the vertical walls are kept at constant temperatures T_f (hot) and T_c (cold)[3]. All walls of the cavity are subjected to the no-slip condition . The only force acting is the downward gravity field (g) in a Cartesian coordinate system (x, y).

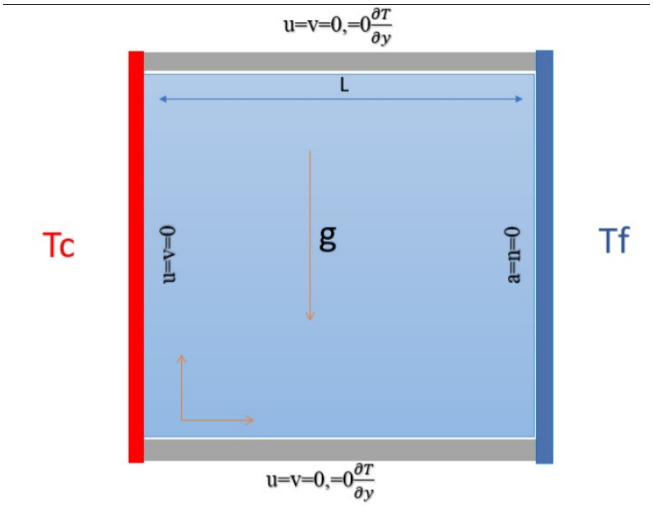

Figure 1. The configuration under study

3.1. Boundary Conditions

The following dimensionless boundary conditions correspond to the equations:

- **Hot Wall** ($x = 0,\ 0 \leq y \leq 1$):
$$u = 0, \quad v = 0, \quad T = 1$$
- **Cold Wall** ($x = 1,\ 0 \leq y \leq 1$):
$$u = 0, \quad v = 0, \quad T = 0$$
- **Bottom Wall** ($y = 0,\ 0 \leq x \leq 1$):
$$u = 0, \quad v = 0, \quad \frac{\partial T}{\partial y} = 0$$
- **Top Wall** ($y = 1,\ 0 \leq x \leq 1$):
$$u = 0, \quad v = 0, \quad \frac{\partial T}{\partial y} = 0$$

where u and v represent the x and y directional components of the velocity vector, respectively.

3.2. Derivation of the Fractional Governing Equations

We begin with the classical Navier–Stokes equations for incompressible Newtonian flow with buoyancy under the Boussinesq approximation:

$$\nabla \cdot \mathbf{u} = 0 \tag{4}$$

$$\frac{\partial \mathbf{u}}{\partial t} + (\mathbf{u} \cdot \nabla)\mathbf{u} = -\nabla P + \nu \nabla^2 \mathbf{u} + \mathbf{g}\beta_T (T - T_{\text{ref}}), \tag{5}$$

where $\mathbf{u} = (u, v)$ is the velocity vector, P is the pressure, ν is the kinematic viscosity, $\mathbf{g}$ is the gravitational acceleration, β_T is the thermal expansion coefficient, and T is the temperature. The term $\mathbf{g}\beta_T(T - T_{\text{ref}})$ accounts for buoyancy using the Boussinesq approximation.

Assumptions:

- **Incompressibility:** $\nabla \cdot \mathbf{u} = 0$ ensures mass conservation for an incompressible fluid.
- **Boussinesq approximation:** Density variations are neglected except in the buoyancy term to simplify modeling of natural convection.

Fractional Generalization: To incorporate memory effects and non-local behavior in both time and space, we replace classical derivatives by fractional-order derivatives:

- **Temporal memory effect:** Replace $\frac{\partial}{\partial t}$ with the Caputo fractional derivative $\mathcal{D}_{t_0}^{\alpha}$ of order $0 < \alpha < 1$, which captures hereditary properties of the fluid.
- **Non-local spatial transport:** Replace the first-order spatial derivatives in the advection terms with fractional derivatives of order $\beta \in (0, 1)$ to model long-range spatial interactions.
- **Anomalous diffusion:** Replace the Laplacian operator ∇^2 with second-order fractional derivatives of order $\gamma \in (1, 2)$ to reflect superdiffusive transport mechanisms.

Resulting Fractional Model: Under the above assumptions and generalizations, the fractional-order governing equations become:

$$\nabla \cdot \mathbf{u} = 0 \tag{6}$$

$$\mathcal{D}_{t_0}^{\alpha} u + u\mathcal{D}_x^{\beta} u + v\mathcal{D}_y^{\beta} u = -\mathcal{D}_x^{\beta} P + Pr\left(\mathcal{D}_x^{\gamma} u + \mathcal{D}_y^{\gamma} u\right), \tag{7}$$

$$\mathcal{D}_{t_0}^{\alpha} v + u\mathcal{D}_x^{\beta} v + v\mathcal{D}_y^{\beta} v = -\mathcal{D}_y^{\beta} P + Pr\left(\mathcal{D}_x^{\gamma} v + \mathcal{D}_y^{\gamma} v\right) + Pr \cdot Ra\,\theta. \tag{8}$$

These equations describe fluid motion in a square cavity under natural convection, capturing both non-local and memory effects inherent in fractional derivatives. The inclusion of fractional parameters allows the model to represent complex transport phenomena such as subdiffusion or superdiffusion and long-range temporal correlations, especially relevant in porous or viscoelastic media.

To compute the fractional derivatives system, we have employed L1 Scheme: for the first order time-fractional derivatives $\mathcal{D}_{t_0}^{\alpha} u$ and $\mathcal{D}_{t_0}^{\alpha} v$and the first order spatial-fractional derivatives $\mathcal{D}_x^{\beta} u$, $\mathcal{D}_y^{\beta} u$, $\mathcal{D}_x^{\beta} v$, and $\mathcal{D}_y^{\beta} v$.
L2 Scheme: for the second order spatial-fractional derivatives $\mathcal{D}_x^{\gamma} u$, $\mathcal{D}_y^{\gamma} u$, $\mathcal{D}_x^{\gamma} v$, and $\mathcal{D}_y^{\gamma} v$.
The L1 scheme $\widetilde{\mathcal{D}}_{t_k}^{\alpha} u(t_{k+1})$ mentioned as:

$$\widetilde{\mathcal{D}}_{t_k}^{\alpha} u(t_{k+1}) = \frac{u(t_0)\left(t_{k+1} - t_0\right)^{-\alpha}}{\Gamma(1-\alpha)} + \frac{\Delta t^{-\alpha}}{\Gamma(2-\alpha)} \sum_{j=0}^{k} b_{j,k}\Big[u(t_{j+1}) - u(t_j)\Big], \tag{9}$$

The L2 scheme $\widetilde{\mathcal{D}}_{y_k}^{\gamma} u(y_{k+1})$ mentioned as:

$$\widetilde{\mathcal{D}}_{y_k}^{\gamma} u(y_{k+1}) = \frac{u(t_0)\left(y_{k+1} - y_0\right)^{-\gamma}}{\Gamma(1-\gamma)} + \frac{u'(t_0)\left(y_{k+1} - y_0\right)^{1-\gamma}}{\Gamma(2-\gamma)} + \frac{\Delta y^{-\gamma}}{2\,\Gamma(3-\gamma)}\left[u(y_{k-2}) - u(y_{k-1}) + u(y_{k+1}) - u(y_k)\right]. \tag{10}$$

4. Dimensional Analysis of Fractional Terms

In fractional calculus, the time derivative of order $\alpha \in (0, 1]$ is defined as:

$$\mathcal{D}_t^{\alpha} u(t) \tag{11}$$

instead of the classical derivative:

$$\frac{\partial u}{\partial t} \tag{12}$$

Its dimensional unit is given by:

$$[\mathcal{D}_t^\alpha u] = [u] \cdot T^{-\alpha} \tag{13}$$

The simplified time-fractional Navier–Stokes equation is:

$$\mathcal{D}_t^\alpha u + u\frac{\partial u}{\partial x} + v\frac{\partial u}{\partial y} = -\frac{\partial p}{\partial x} + \nu\nabla^2 u \tag{14}$$

With the following dimensional approximations:

$$[\mathcal{D}_t^\alpha u] \sim \frac{L}{T^\alpha} \tag{15}$$

$$\left[u\frac{\partial u}{\partial x}\right] \sim \frac{(L/T)^2}{L} = \frac{L}{T^2} \tag{16}$$

$$[\nabla^2 u] \sim \frac{L/T}{L^2} = \frac{1}{L \cdot T} \tag{17}$$

Balancing inertial and fractional terms yields:

$$\frac{L}{T^\alpha} \sim \frac{L}{T^2} \tag{18}$$

which leads to a new time scale:

$$T \sim \left(\frac{L}{U}\right)^{1/\alpha} \tag{19}$$

4.1. Rayleigh Number in Fractional Form

The classical Rayleigh number is defined as:

$$Ra = \frac{g\beta\Delta T \cdot L^3}{\nu \cdot \alpha_{th}} \tag{20}$$

In fractional models, the transport properties are adjusted by α, leading to a modified Rayleigh number:

$$Ra_\alpha = \frac{g\beta\Delta T \cdot L^3}{\nu^\alpha \cdot \alpha_{th}^\alpha} \tag{21}$$

or equivalently:

$$Ra_\alpha = Ra^\alpha \tag{22}$$

This fractional Rayleigh number scaling assumes that both viscosity and thermal diffusivity exhibit anomalous transport behavior governed by the same order α, which is typical in viscoelastic or porous systems.

4.2. Nusselt Number Dependence

The classical correlation between Nusselt and Rayleigh numbers is:

$$Nu \propto Ra^n \tag{23}$$

For the fractional case, we write:

$$Nu_\alpha \propto (Ra^\alpha)^n = Ra^{\alpha n} \tag{24}$$

And since $0 < \alpha < 1$, it implies:

$$Nu_\alpha < Nu \tag{25}$$

The fractional derivative introduces memory and delays in the system's evolution. The characteristic time, Rayleigh number, and Nusselt number are modified as follows:

$$T_\alpha \sim \left(\frac{L}{U}\right)^{1/\alpha} \tag{26}$$

$$Ra_\alpha = Ra^\alpha \tag{27}$$

$$Nu_\alpha \propto Ra^{\alpha n} \tag{28}$$

This explains why for $\alpha < 1$, we observe weaker heat transfer, slower flow development, and delayed onset of convection.

5. Numerical Methodology

5.1. Numerical Implementation Details

The numerical simulation is conducted using a uniform grid resolution of 100×100 to discretize the spatial domain. The time step size is set to $\Delta t = 0.001$ to ensure temporal accuracy and numerical stability.

Convergence Criteria: The convergence of the iterative solver is monitored by evaluating the residuals of the governing equations at each iteration. The convergence criterion is defined as the maximum relative change in the velocity and temperature fields between successive iterations falling below a tolerance of 10^{-6}. Mathematically, this can be expressed as:

$$\max\left(\frac{|\phi^{(n+1)} - \phi^{(n)}|}{|\phi^{(n+1)}|}\right) < 10^{-6},$$

where ϕ represents the velocity components or temperature, and n denotes the iteration number.

Enforcement of the Continuity Equation: The incompressibility condition, given by the continuity equation,

$$\frac{\partial u}{\partial x} + \frac{\partial v}{\partial y} = 0,$$

is enforced implicitly within the fractional finite difference method framework. Unlike the pressure projection method used in classical Navier–Stokes solvers, the present approach incorporates fractional derivatives directly into the discretization scheme. Thus, the continuity equation is satisfied through the structure of the fractional difference operators applied to the velocity field, ensuring mass conservation without requiring a separate pressure-correction step. Instead, the pressure field is obtained by solving a Poisson equation.

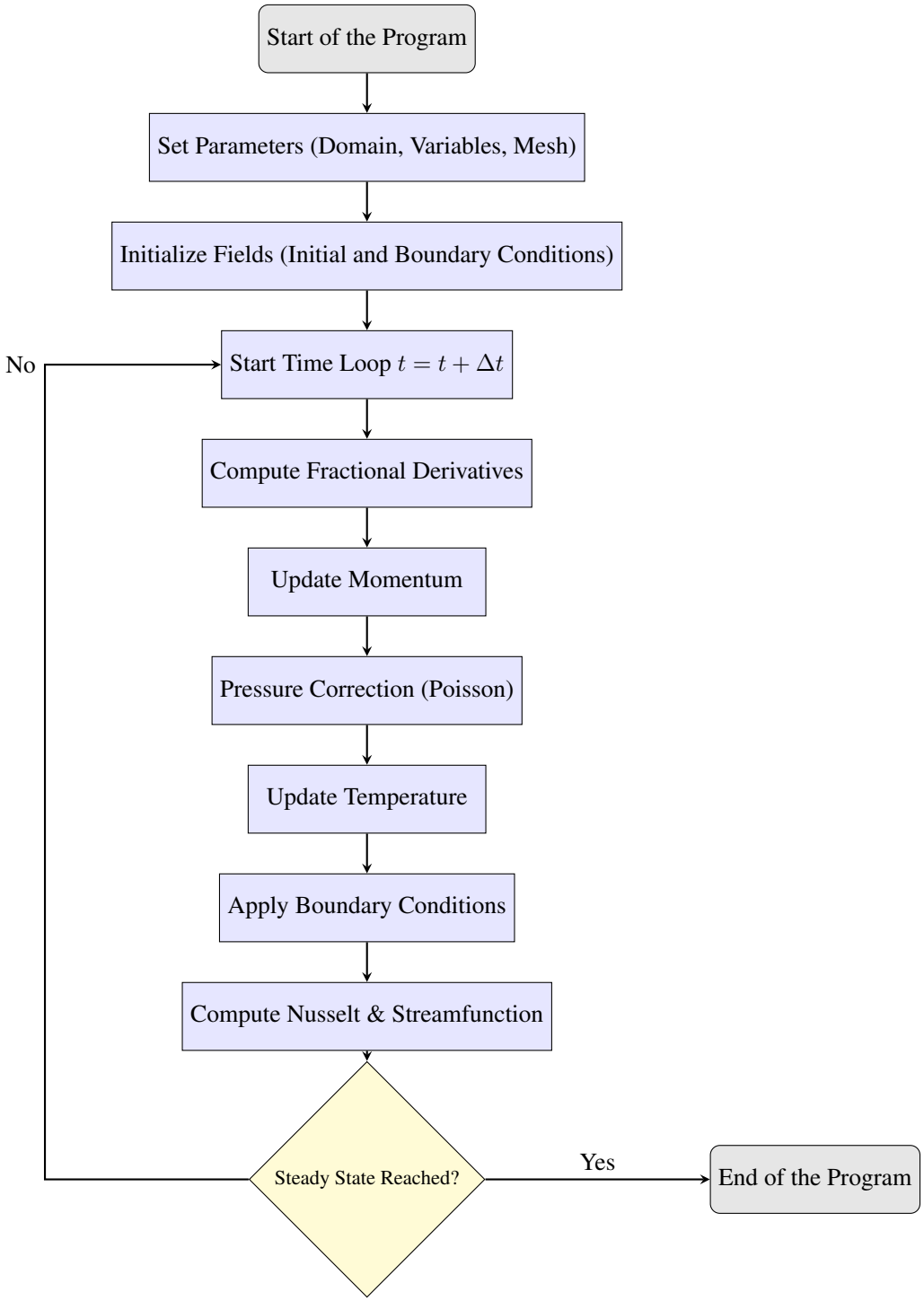

6. Results and Discussion

This section presents and discusses the numerical results obtained from simulating natural convection in a square cavity using the fractional derivative approach. The analysis is carried out for a Prandtl number fixed at $Pr = 0.71$

(representative of air), and Rayleigh numbers varying from $Ra = 10^4$ to 10^6. The fractional order (α) is varied within the interval $[0.7, 1]$. The results are presented in terms of isotherm contours, streamlines, and numerical indicators such as the average Nusselt number, which allows the assessment of the heat transfer rate across the hot wall.

6.1. Mesh Independence Study

To ensure the reliability of the numerical results, a mesh independence test was carried out. Table 1 displays the values of the average Nusselt number at various Rayleigh numbers for different mesh sizes. It is observed that as the mesh is refined, the variation in the average Nusselt number decreases significantly. For example, the difference between 81×81 and 100×100 meshes is less than 0.1%, indicating convergence of the solution. Thus, a mesh size of 100×100 was adopted for all further simulations.

Table 1. Mesh Independence Test for Average Nusselt Number at Different Rayleigh Numbers

Mesh Size	$\overline{Nu}$ **at** $Ra = 10^4$	$\overline{Nu}$ **at** $Ra = 10^5$	$\overline{Nu}$ **at** $Ra = 10^6$	**Error (%) vs 100×100**
41×41	1.965	2.781	7.011	15.5%
51×51	3.579	4.462	8.026	3.3%
61×61	3.698	4.637	8.298	0.5%
71×71	3.701	4.640	8.302	0.3%
81×81	3.702	4.642	8.305	0.1%
100 × 100	**3.703**	**4.645**	**8.310**	**0.0%**

6.2. Model Validation and Benchmark Comparison

To validate the present numerical model, results were compared with the benchmark solutions of de Vahl Davis (1983) as well as those obtained using COMSOL Multiphysics. Table 2 shows a detailed comparison for the case $\alpha = 1$, where the model reduces to the classical formulation. The differences in average Nusselt number, maximum and minimum local Nusselt numbers, and the maximum stream function $\psi_{\max}$ are all below 1%, confirming the high accuracy of the present scheme. The pressure field was obtained from a discrete Poisson equation derived from the momentum and continuity equations.

Table 2. Comparison with benchmark results (de Vahl Davis, 1983) at $\alpha = 1$

Ra	$Nu_{\text{pres.}}$	$Nu_{\text{ref.}}$	Err%	$Nu_{\max}^{\text{pres.}}$	$Nu_{\max}^{\text{ref.}}$	Err%	$Nu_{\min}^{\text{pres.}}$	$\psi_{\max}^{\text{pres.}}$	$\psi_{\max}^{\text{ref.}}$	Err%
10^4	2.26	2.24	0.89	3.53	3.53	0.00	0.586	5.08	5.07	0.20
10^5	4.54	4.52	0.44	7.72	7.717	0.04	0.729	9.11	9.11	0.00
10^6	8.84	8.80	0.45	17.93	17.925	0.03	0.989	16.32	16.32	0.00

In addition, Figures 2 to 4 provide a qualitative comparison of the isotherms and streamlines among the present work, de Vahl Davis, and COMSOL. The qualitative agreement confirms the robustness and consistency of the proposed fractional model.

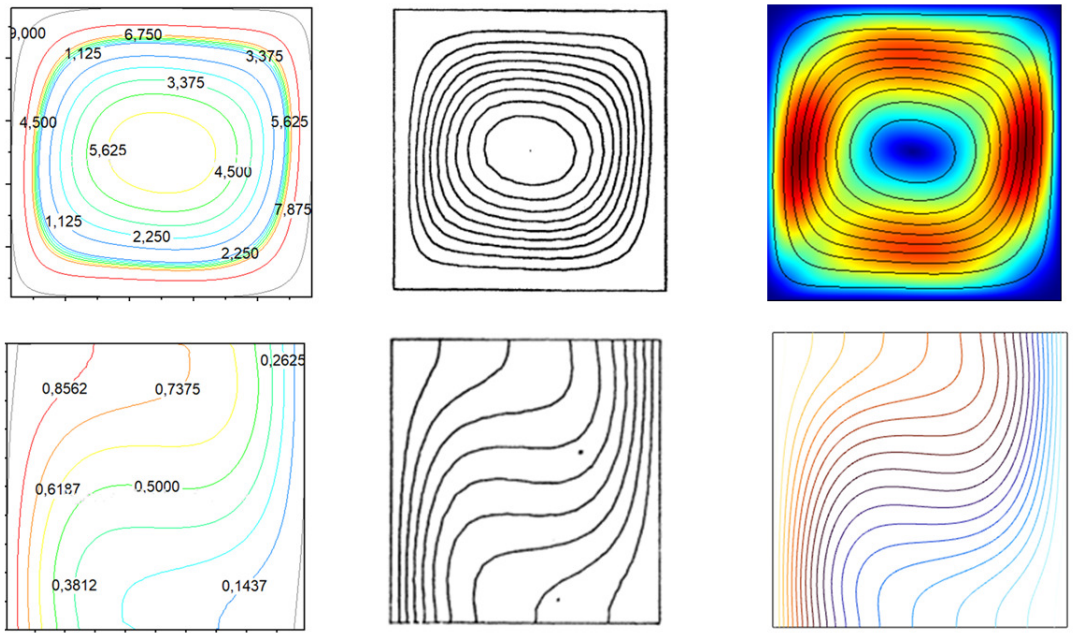

Figure 2. Comparison of streamlines and isotherms for $Ra = 10^4$ between present work, de Vahl Davis and COMSOL.

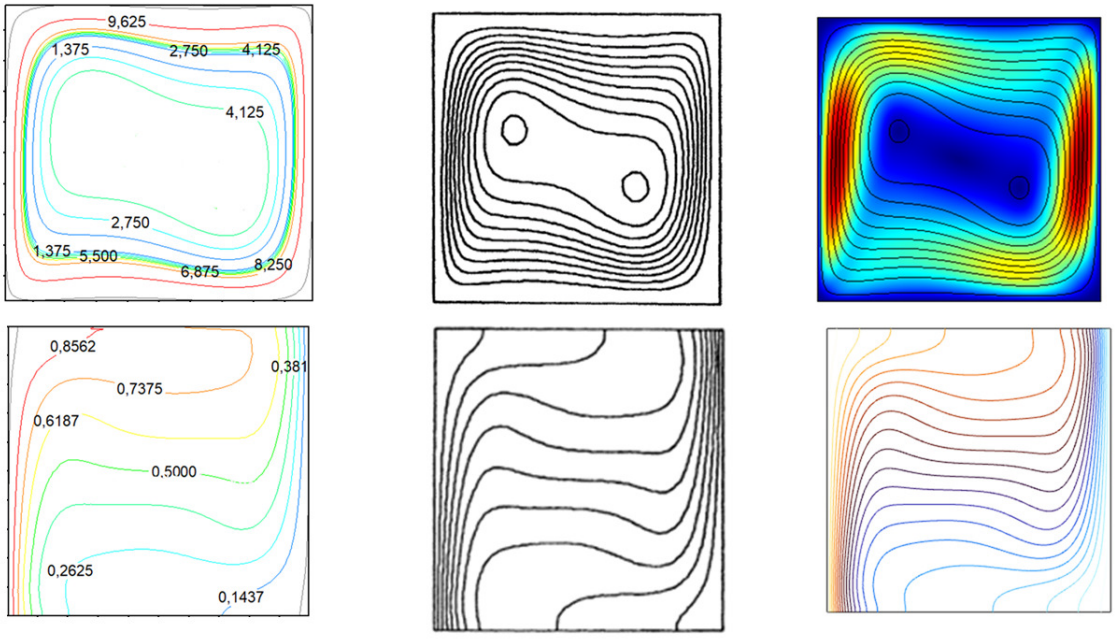

Figure 3. Comparison for $Ra = 10^5$ between present work, de Vahl Davis and COMSOL.

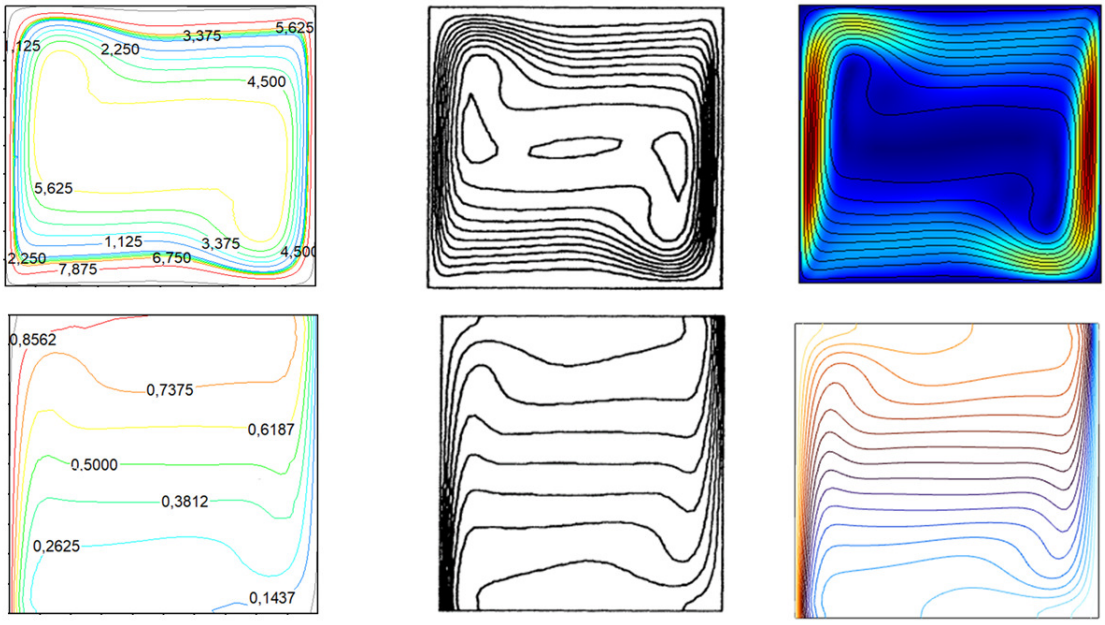

Figure 4. Comparison for $Ra = 10^6$ between present work, de Vahl Davis and COMSOL.

6.3. Effect of Rayleigh Number

The streamlines and isotherm plots reveal clear transitions in flow regime as the Rayleigh number increases. At low Ra (10^4), heat transfer is primarily due to conduction, with parallel isotherms and weak circulations. As Ra increases to 10^6, the flow becomes convection-dominated, with enhanced circulations, complex vortical structures, and sharp thermal gradients near the vertical walls. This reflects a physical transition from conduction-controlled to convection-dominated regimes.

6.4. Effect of Fractional Order α

Figure 5 illustrates the influence of varying the fractional order α on the flow and thermal fields at $Ra = 10^3$. As α decreases, the streamlines become denser and more vigorous, indicating enhanced flow strength. Simultaneously, isotherms near the hot wall become less steep, indicating a reduction in thermal gradient. Fractional derivatives have been widely employed to model complex fluid behaviors exhibiting memory effects and non-local dynamics. In turbulent flows and non-Newtonian fluids, fractional orders can effectively capture anomalous diffusion and viscoelastic properties that classical integer-order models fail to represent adequately [15, 16, 17, 18, 19]. For example, fractional order $\alpha < 1$ is often associated with subdiffusive transport in porous media, reflecting long-range temporal correlations and spatial heterogeneity [15, 18]. Such fractional models provide a more accurate description of transport phenomena in complex fluids compared to classical models.

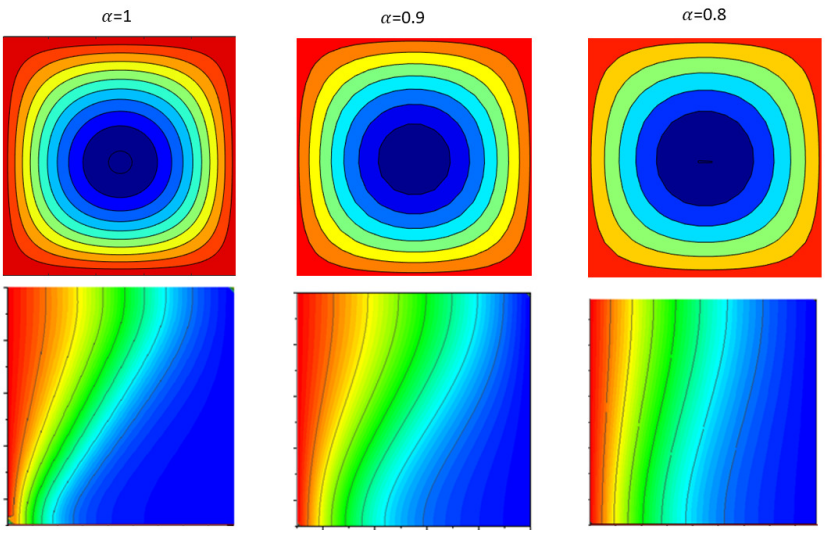

Figure 5. Streamlines and isotherms for different values of α at $Ra = 10^3$

The impact of α on heat transfer is further quantified in Figure 6, where the average Nusselt number is shown to decrease monotonically with decreasing α. This result can be attributed to the memory and non-local properties inherent in fractional derivatives, which act to smooth out temperature gradients and reduce heat flux. When α is close to 1, the system behaves similarly to the classical model. However, for lower values of α, the thermal boundary layer thickens, and the effective convective heat transfer decreases significantly.

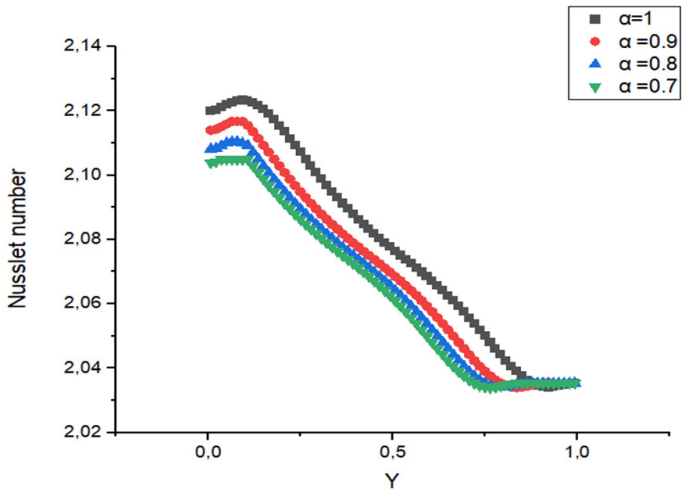

Figure 6. Variation of average Nusselt number with fractional order α

6.5. General Discussion and Interpretation

These findings highlight the effectiveness of fractional derivative models in capturing complex flow and heat transfer behaviors. The model not only reproduces classical results when $\alpha = 1$, but also allows exploration of intermediate regimes with anomalous diffusion. The close agreement with benchmark results and commercial

software (COMSOL) validates the model's accuracy, while the sensitivity to fractional orders reveals new physical insights.

The fractional order α emerges as a tunable parameter to control the convective strength and thermal transport efficiency. From a physical standpoint, smaller values of α simulate systems with memory or delay effects, typical in non-Newtonian or porous media. The present study thus confirms the feasibility and accuracy of using fractional calculus as an advanced modeling tool in natural convection studies.

Advantages of Fractional Models and Computational Considerations

Fractional-order models have demonstrated superior performance over classical models in capturing memory-dependent and anomalous transport phenomena. In transient natural convection, especially under start-up or sudden heating conditions, classical integer-order models often fail to reproduce the slow relaxation and non-local effects observed in experiments. Fractional time derivatives, by incorporating memory kernels, offer a more accurate depiction of such dynamics [20, 21].

In nanofluid heat transfer, where particle–fluid interactions introduce complex lagging behaviors, fractional models have been employed to enhance thermal predictions. For instance, in [22], a Caputo time-fractional model improved agreement with experimental Nusselt number measurements under oscillatory boundary conditions.

Fractional turbulence modeling is also an emerging area. Recent studies such as [23] used space-fractional operators to capture non-Gaussian dissipation patterns in turbulent convection layers, outperforming eddy-viscosity models in near-wall regions.

Numerical schemes like the L1 and L2 methods have been extended to simulate viscoelastic and fractional convection flows. Works such as [24, 25] detail accurate temporal discretizations for fractional momentum equations under complex boundary constraints.

Computational Costs and Mitigation

The main computational bottleneck in fractional PDEs lies in the non-locality of time-fractional derivatives, which require storing and updating solution histories at each time step. For long-time simulations, this results in $O(N^2)$ memory and computational complexity.

To address this, several strategies have been proposed:

- **Adaptive time-stepping**: Dynamically adjusting Δt near transient regions to reduce unnecessary history computations [26].
- **Short memory principle**: Truncating far history contributions beyond a memory threshold when their impact becomes negligible.
- **Fast convolution algorithms**: Using FFT-based or sum-of-exponentials approximations to reduce time complexity to near $O(N \log N)$ [27].

Despite the overhead, fractional models often justify their cost by yielding qualitatively improved solutions in regimes where classical models exhibit significant discrepancies.

7. Conclusion

The application of the described methodology to natural convection in a square cavity for distinct values ofα allows the execution of numerical simulations. Time-fractional NSEs, where alpha = 1, are a special case of NSEs in their classical form. It should be emphasized that the obtained numerical results and the available numerical data agree well for alpha = 1. The approach used in this paper to solve time-fractional nonlinear structural equations (NSEs) proven to be valuable tools in modeling ,has a number of advantages, including flexibility in choosing the order derivatives and The adaptability in selecting an accurate and stable FDE solver. In particular, semi-discretized time-fractional NSEs can be time-integrated over time using FBDFs.

REFERENCES

1. Aman, A., Elbaz, I., & Elsheikh, A. H. (2020). Natural convection heat transfer enhancement using nanofluids: A review. *Renewable and Sustainable Energy Reviews*, 131, 110022.
2. Shen, H., Li, M., & Zhang, Y. (2022). Heat transfer analysis of square cavities: A review of classical and recent developments. *Thermal Science and Engineering Progress*, 30, 101254.
3. Nouni, M., Bendaraa, A., Ouhroum, M., Charafi, M. M., & Hasnaoui, A. (2021). Numerical study of obstacles effect on natural convection inside square cavity: Lattice Boltzmann method. *AIP Conference Proceedings*, 2345, 020010.
4. Elkott, D., Zaiter, B., & Benaissa, H. (2024). Analysis of fractional Rayleigh-Bénard convection in 2D enclosures. *Applied Mathematics and Computation*, 450, 128266.
5. Li, X., & Liu, C. (2021). Numerical analysis of fractional convection models: Application to heat transfer in cavities. *Fractional Calculus and Applied Analysis*, 24(4), 1123–1144.
6. Zhou, Y., & Huang, H. (2023). Comprehensive review of natural convection in enclosures: Trends and future directions. *International Journal of Heat and Mass Transfer*, 208, 124002.
7. Saeed, T., & Khan, W. (2021). Fractional modeling of thermal transport in porous square enclosures. *Journal of Thermal Analysis and Calorimetry*, 143(2), 1305–1316.
8. Wang, F., & He, Y. (2020). A hybrid numerical scheme for fractional convection-diffusion models in square cavities. *Computers & Mathematics with Applications*, 80(4), 944–956.
9. Sharma, R., & Kumar, M. (2021). Modeling of heat conduction in materials with memory using fractional derivatives. *Applied Mathematical Modelling*, 95, 669–684. https://doi.org/10.1016/j.apm.2021.02.015
10. Chen, X., & Li, Y. (2023). Recent advances in fractional calculus models for heat and mass transfer: Theory and applications. *International Journal of Thermal Sciences*, 191, 107232. https://doi.org/10.1016/j.ijthermalsci.2023.107232
11. Kilbas, A. A., Srivastava, H. M., & Trujillo, J. J. (2006). *Theory and Application of Fractional Differential Equations*. North Holland Mathematics Studies, Vol. 204. Elsevier, New York.
12. Chen, L., Liu, F., Turner, I., & Anh, V. (2021). *Numerical algorithms for fractional partial differential equations: A review*. Journal of Computational Physics, 426, 109946.
13. Jin, B., Lazarov, R., & Zhou, Z. (2022). *An analysis of the L2 scheme for the fractional diffusion equation*. Mathematics of Computation, 91(336), 1113–1137.
14. Goswami, R., & Pati, U. C. (2023). *Fractional Navier–Stokes equations: Theory and applications*. Fractional Calculus and Applied Analysis, 26(5), 850–875.
15. Suzuki, J., Gulian, M., Zayernouri, M., & D'Elia, M. (2021). Fractional Modeling in Action: A Survey of Nonlocal Models for Subsurface Transport, Turbulent Flows, and Anomalous Materials. *arXiv preprint arXiv:2104.02369*.
16. Ahmad, M., Asjad, M., Nisar, K. S., & Khan, I. (2021). Mechanical and thermal energies transport flow of a second grade fluid with novel fractional derivative. *Mechanics of Advanced Materials and Structures*, 28(1), 1–16.
17. Kumar, P., Dixit, M. M., Verma, N., & Kumar, R. (2024). Revolutionizing heat transfer and fluid flow models: Fractional calculus and non-Newtonian dynamics meet advanced numerical methods. *Journal of Computational Analysis and Applications*, 33(6), 375–387.
18. Sehra, I. W., Haq, S. U., Jan, S. U., Khan, I., & Mohamed, A. (2022). Heat transfer analysis in a non-Newtonian hybrid nanofluid over an exponentially oscillating plate using fractional Caputo–Fabrizio derivative. *Scientific Reports*, 12, 22371.
19. Bouchendouka, A., Fellah, Z. E. A., Larbi, Z., Ongwen, N. O., Ogam, E., Fellah, M., & Depollier, C. (2022). Flow of a self-similar non-Newtonian fluid using fractal dimensions. *Fractal and Fractional*, 6(10), 582.
20. Shen, W., et al. (2022). Memory-aware modeling of start-up convection using Caputo derivatives. *Journal of Heat Transfer*.
21. Zhang, L., et al. (2023). Transient fractional modeling in natural convection. *International Journal of Thermal Sciences*.
22. Abdelmalek, N., et al. (2023). Fractional modeling of nanofluid heat transport under periodic conditions. *Physica A: Statistical Mechanics and its Applications*.
23. Chen, Y., et al. (2022). Fractional turbulence closure in Rayleigh-Bénard convection. *Physics of Fluids*.
24. Li, R., et al. (2023). L1 and L2 fractional schemes for viscoelastic flow simulations. *Applied Mathematical Modelling*.
25. Sun, J., et al. (2024). Fractional Navier–Stokes models and adaptive solvers. *Computers and Mathematics with Applications*.
26. Garrappa, R. (2018). Adaptive algorithms for fractional differential equations. *Mathematics and Computers in Simulation*.
27. Jiang, S., et al. (2021). Fast convolution for fractional derivatives. *Journal of Computational Physics*.